Angewandte Chemie

Shape-Memory Polymers

DOI: 10.1002/ange.201103908

Nanoparticle Netpoints for Shape-Memory Polymers**

*Praveen Agarwal, Madhur Chopra, and Lynden A. Archer**

Shape-memory polymers (SMPs)[1,2] are a class of stimuli-responsive materials[3] which have the capacity to remember a pre-programmed shape imprinted during synthesis; can be reformed at a higher temperature to impart a desired temporary shape; and recover their original shape when acted upon by a stimulus, for example, heat, light, or magnetic field. Conventionally, addition of nanoparticles as fillers in SMPs has been reported to improve their mechanical properties, but typically at the expense of shape-memory performance and with the result of a broadened transition temperature.[4–7] Herein we report a new family of hybrid inorganic–organic SMPs employing inorganic nanoparticles as netpoints. In these materials, each netpoint is a junction for hundreds of polymer chains. We find that this network design leads to dramatic increases in the elastic modulus without the typical loss of sharpness in the transition temperature and excellent shape-memory properties. Significantly, because the netpoints are functional inorganic nanostructures, the new design opens the way for synthesis of multifunctional SMPs with tunable physical properties and transition temperatures.

SMPs are attractive for a growing list of applications—from smart sutures and implants for minimally invasive surgery, to responsive, shape-shifting optical components.[1,2,4–8] Advantages that SMPs present over shape-memory metal alloys[9,10] range from their low density, more accessible and tailorable switching temperatures, lower cost, and flexibility.[1–8] A typical disadvantage of SMPs as compared to shape-memory alloys is their low stress generation owing to their generally lower, polymeric elastic modulus.[2,4,5] There have been few reports on approaches for producing stronger SMPs,[11–13] but these efforts are insufficient to provide a versatile platform for synthesizing SMPs with desired properties and multifunctionality[14–20] at the same time.

SMPs typically consist of two elements: netpoints and switching segments.[1,2] Netpoints are typically the connection points for polymer chains in a network and are responsible for determining the permanent shape of the material. The switching segments are polymer chains incorporated into the network, which are responsible for the shape-memory effect owing to the entropic elasticity of these chains. Netpoints can be chemical in nature, as in covalently connected polymer segments in cross-linked networks. They can also exist as physical cross-links, as has been realized in block-copolymer-based SMPs.[1,2] For most reported covalent SMP networks, netpoints are of molecular size; a few known exceptions are from the report by Xu and Song,[21] where SMPs based on polyhedral oligosilsesquioxane (POSS) cores were demonstrated and from the work by Cao and Jana,[22] where nanoclay-tethered SMPs were reported.

Recently we reported on a novel family of organic–inorganic hybrids called nanoscale ionic materials (NIMs).[23–26] Created by densely grafting functional oligomer chains (corona) to nanoparticle cores, these materials display fluidlike properties in the absence of any external solvent and have been termed self-suspended suspensions.[23,24] Physical properties of these materials such as viscosity, elastic modulus, and glass-transition and melting temperature can be facilely tuned by systematically changing the core volume fraction, corona molecular weight, and grafting density.[23–26] Materials created from different nanoparticle core chemistry, size, and shape have already been reported.[23–26]

We synthesized the hybrid polymeric networks by interconnecting the free ends of the NIMs' corona. We demonstrate hybrid SMPs herein using the simplest configuration, NIMs comprised of a SiO_2 core and polyethylene glycol (PEG) corona. A perhaps obvious advantage of these materials is that the inherent biocompatibility of the PEG corona[27] and silica[28] cores immediately renders them attractive candidates for biomedical applications. In the synthesis scheme, silica nanoparticles are first grafted with sulfonic acid groups using the reported procedure.[23,25] The resultant sulfonic acid functionalized particles are subsequently treated with dual-functional PEG chains containing amine and hydroxy end groups. The tethered sulfonic acid reacts selectively with the amine groups to produce nanoparticles with hydroxy groups at the ends of tethered PEG chains (Figure 1 a). As shown in Figure 1 b, reaction of these particles with hexamethylene diisocyanate (HDI) yields cross-linked polymer networks in which the SiO_2 cores of the NIMs are the netpoints. We have shown previously that densely functionalized nanostructures comprised of as many as 1–2 polymer chains nm^{-2} can be created using this approach,[23] which translates up to 300–600 chains per particle for the 10 nm particle size use in this study. As illustrated in Figure 1 c, these materials manifest shape-memory properties, in that they can be cooled to remember their shape and when heated again, they quickly recover their original, fixed shape.

Figure 2 a shows the storage modulus versus temperature for samples created using PEG with corona molecular weight of 5000 $g\,mol^{-1}$ and polydispersity index $M_w/M_n = 1.06$. The inorganic content of the materials can be simply tuned by changing the number of polymer chains attached to each

---

[*] P. Agarwal, M. Chopra, Prof. L. A. Archer
Department of Chemical and Biomolecular Engineering
Cornell University, Ithaca, NY 14850 (USA)
E-mail: laa25@cornell.edu

[**] This work was supported by Award No. KUS-C1-018-02, made by King Abdullah University of Science and Technology (KAUST), and by the National Science Foundation, Award No. DMR-1006323. Facilities available though the Cornell Center for Materials Research (CCMR) were used for this study.

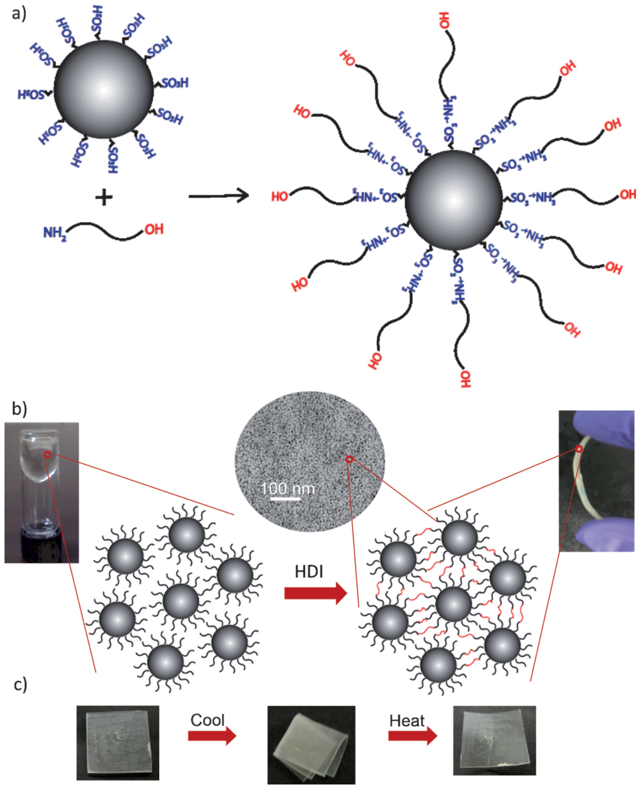

Figure 1. a) Schematic depiction of the reaction scheme. b) Transformation of un-cross-linked, liquidlike NIMs (left) into cross-linked solid SMP hybrids (right). The TEM image of the SMP (center) shows that the nanoparticles are well dispersed and that the size of the silica nanoparticles is 10 nm. c) Pictures showing shape fixing (at −10 °C) and recovery (at 60 °C).

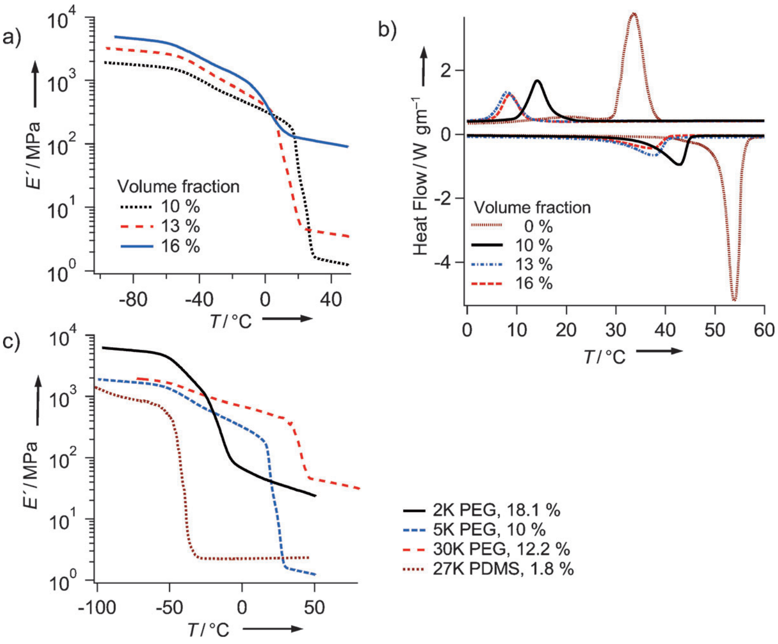

Figure 2. a) Elastic modulus *E*′ vs. temperature for the SiO_2–PEG SMP samples with corona molecular weight of 5000 and varying particle volume fraction. b) DSC traces for the samples in (a) and also of unattached NH_2- and OH-terminated PEG. c) Elastic modulus versus temperature for the hybrid SMPs created with varying corona chemistry, molecular weight, and particle content. Here, the symbol K represents 1000 g mol^{-1}.

particle and characterized by thermogravimetric analysis (TGA). It is readily apparent from Figure 2 a that the addition of particles results in a significant increase in both the rubbery and glassy moduli, and that there is a systematic increase with increasing inorganic particle volume fraction. At a moderate particle volume fraction of 0.16, the rubbery modulus of the material is of order 100 MPa at room temperature, which is substantially higher than reported for SMP composites, where the typical value of the rubbery modulus is in the range of 1–10 MPa.[6,7]

Figure 2 b shows differential scanning calorimetry (DSC) traces for the same samples and also the untethered PEG. These results indicate that the transition temperature T_{trans} for the material is associated with the melt/crystallization transition of PEG[29] chains anchored to the netpoints. During the cooling cycle, crystallization takes place between 10 and 15 °C and during the heating cycle, the melting transition appears within the temperature range of 35–45 °C, that is, close to physiological temperatures. These results compare well with typical transition temperatures (20–80 °C) for reported SMPs.[1,2] As evident from both dynamic mechanical analysis (DMA) and DSC results, the transition from a rubbery state to a glassy state is very sharp in our materials. This observation is important, because a sharp transition temperature is crucial for quick shape recovery and fixity; it could be contrasted with the broad distribution of transition temperatures reported for SMP nanocomposites.[4,6,7] DSC results also indicate that addition of particles leads to a reduction in the transition temperature and crystallinity of the hybrid SMP as compared to the free polymer, which could possibly be explained by the fact that polymer chains are more constrained owing to immobilization of both chain ends.

Figure 2 c shows the DMA results for hybrid SMPs created using a range of corona molecular weight and chemistry. It can be clearly seen that the modulus and transition-temperature values can be tuned over a wide range by changing the corona molecular weight, chemistry and particle content. Figure 2 c also shows that the corona chemistry is not limited to PEG-based materials; particularly SMPs based on polydimethylsiloxane (PDMS) are possible. It is apparent from Figure 2 c that both the storage modulus and transition temperature can be tailored by changing the corona chain molecular weight or chemistry. For the PEG-based materials, the transition temperature corresponds to the melting transition, whereas for the PDMS-based materials, the transition corresponds to the glass transition.

SMP composites have been reported to suffer from deteriorated shape-memory performance upon addition of fillers.[7] This effect has been speculated to stem from structural defects in the network produced by the fillers, which reduces the network homogeneity and strand connectivity. This drawback is not seen in the hybrid SMPs reported herein, presumably because the very nanoparticles that provide mechanical reinforce-

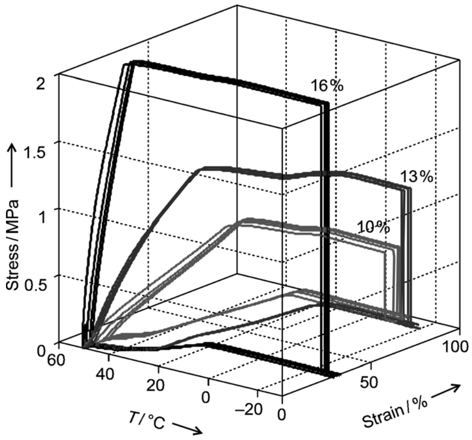

Figure 3. Cyclic thermomechanical tensile test results for SiO_2 PEG hybrids with variable core volume fraction. Molecular weight of the polymer chain is 5000 $g\,mol^{-1}$.

ment act as netpoints for the cross-linked networks. We have characterized the shape-memory performance of the materials shown in Figure 2a using cyclic thermomechanical tests as shown in Figure 3. In these tests, the material is first stretched at a temperature higher than T_{trans} and then cooled below T_{trans} at fixed stress to fix the shape. Stress is then reduced to zero and the strain decay during this step is used to characterize the shape fixity. It is apparent from Figure 3 that there is no noticeable decay in the strain, implying that these materials have good shape fixity. For the recovery, the material is heated to a temperature above T_{trans}, and its shape recovery is characterized by the corresponding strain recovery under stress-free conditions. It can be seen from Figure 3 that during this process, the strain recovers almost fully, thus implying that these materials are able to recover to their original shape. This process is repeated for multiple cycles, nicely demonstrating that the materials possess good shape fixity and recovery after multiple cycles of loading and unloading. Values for the shape fixity and recovery ratios for the investigated materials are reported in Table 1. It can be seen that both of the ratios are close to 100 %, which can be contrasted with the low values typically reported for SMP composites, which range from 50 to 90 %.[7]

In conclusion, we have presented a new materials platform for synthesizing hybrid organic–inorganic hybrid shape–memory polymers. The materials incorporate nanoparticles as netpoints in a cross-linked polymer network and thereby appear to overcome many of the shortcomings of conventional hybrid SMPs created by physical dispersion of nanostructures or filler particles in polymer networks. This change leads to significant increases in the elastic modulus, sharp transition temperatures, and excellent shape-memory properties. We attribute these benefits to the fact that issues stemming from immiscibility of filler nanoparticles in the polymer matrix are inherently avoided by tethering the polymers to the nanoparticle core. These materials open up the potential for strong, biocompatible SMPs with continuously tunable mechanical properties and transition temperatures as well as high shape-memory performance. Furthermore, by taking advantage of the large available libraries of nanoparticle shapes, sizes, chemistries, and mass distributions (e.g. hollow, rattles, core–shell),[30] our materials provide a versatile framework for creating SMPs with multifunctional features like remote actuation, biodegradability, and therapeutic release capabilities.[14–20]

Experimental Section

Synthesis of end-functionalized NIMs: Commercially available silica nanoparticle suspensions (LUDOX-SM30, Sigma Aldrich) were diluted and used to synthesize sulfonic acid functionalized nanoparticles using the reported procedure.[25] α-Amino-ω-hydroxy-terminated PEG (Polymer Source Inc.) was added to the resultant sulfonic acid functionalized particles and the mixture was allowed to react for a period of three to four days at room temperature. The amine end groups of the polymer react with the sulfonic acid groups on the particles, and the product contains PEG-tethered silica nanoparticles with a free hydroxy group at the chain end. The product from this reaction was dried and the excess polymer removed by repeated precipitation from chloroform using hexane. To synthesize hybrid SMPs using PDMS, a similar method was employed with a diamino-functionalized PDMS (Sigma Aldrich), and the purification was carried out by precipitation with methanol. The inorganic particle weight fraction in all materials was characterized by thermogravimetric analysis (TGA).

Synthesis of SMPs: To create SMPs with silica nanoparticles as netpoints, the purified product from the preceding steps was dissolved in chloroform and treated with excess hexamethylene diisocyanate (HDI, Sigma Aldrich) to cross-link the tethered polymer chains. The resultant solution was poured into Teflon molds, and the solvent was evaporated by slow heating at 70 °C.

SMP characterization: Rectangular films cut from the material produced in the preceding step were used to measure the elastic modulus as a function of temperature. In a typical experiment, the material was cooled at a rate of 3 °C min^{-1} and a small deformation was applied at a frequency of 1 Hz. DSC was performed in a heat–cool–heat cycle at a heating and cooling rate of 5 °C min^{-1} in a temperature range of 100 to −50 °C. Shape-memory performance was evaluated using a cyclic thermomechanical test performed in the stress-control mode. In this test, samples were stretched up to a specified strain at 50 °C and the stress was kept constant as the sample was cooled to −20 °C (10% and 13% samples) or −30 °C (16% sample). The shape fixity was evaluated from the decrease in the value of strain under stress-free conditions. Shape recovery was quantified from the recovery of strain during heating to 50 °C under stress-free conditions.

Instrumentation: DMA was performed using a TA instrument model Q800 tensile tester outfitted with a tension clamp. DSC experiments were carried out using a

Table 1: Physical properties of samples reported in Figure 2a,b and Figure 3.[a]

ϕ [%]	T_c [°C]	T_m [°C]	E_g [GPa]	E_r [MPa]	R_f [%]	R_r [%]	σ_r [MPa] (50 °C)	ε_r [%] (50 °C)	σ_r [MPa] (0 °C)	ε_r [%] (0 °C)
10	15	43	1.9	1.6	98.5	98.3	0.48	223	8.3	7.1
13	8	38	3.2	4.9	99.5	99.4	3.0	207	9.0	16.1
16	8	37	4.8	126	97.0	96.8	8.8	95	11.5	25

[a] ϕ is the volume fraction of silica nanoparticles. T_c is the crystallization temperature of PEG chains determined from DSC. T_m is the melting temperature of PEG chains determined from DSC. E_g is the glassy modulus determined from DMA. E_r is the rubbery modulus determined from DMA. R_f is the shape fixity ratio. R_r is the shape recovery ratio. σ_r is the stress at break. ε_r is the elongation at break.

TA instruments model Q2000 differential scanning calorimeter based on a heat–cool–heat cycle with liquid nitrogen as coolant. TGA was performed using TA instruments model Q5000 under nitrogen flow. To facilitate TEM imaging, samples were sectioned using a Leica Ultracut-UCT microtome and, TEM was performed using FEI Technai T12 at 120 kV.

Received: February 14, 2011

Keywords: mechanical properties · nanoparticles · organic–inorganic hybrid composites · shape-memory polymers

---

[1] A. Lendlein, A. M. Scmidt, R. Langer, *Proc. Natl. Acad. Sci. USA* **2001**, *98*, 842; A. Lendlein, S. Kelch, *Angew. Chem.* **2002**, *114*, 2138; *Angew. Chem. Int. Ed.* **2002**, *41*, 2034.
[2] C. Liu, H. Qin, P. T. Mather, *J. Mater. Chem.* **2007**, *17*, 1543; P. T. Mather, X. Luo, R. Rousseau, *Annu. Rev. Mater. Res.* **2009**, *39*, 441.
[3] M. A. Cohen Stuart, W. T. S. Huck, J. Genzer, M. Müller, C. Ober, M. Stamm, G. B. Sukhorukov, I. Szleifer, V. V. Tsukruk, M. Urban, F. Winnik, S. Zauscher, I. Luzinov, S. Minko, *Nat. Mater.* **2010**, *9*, 101.
[4] P. Miaudet, A. Derré, M. Maugey, C. Zakri, P. M. Piccione, R. Inoubli, P. Poulin, *Science* **2007**, *318*, 1294.
[5] X. Luo, P. T. Mather, *Soft Matter* **2010**, *6*, 214.
[6] Y. Liu, K. Gall, M. L. Dunn, P. McCluskey, *Mech. Mater.* **2004**, *36*, 929.
[7] S. A. Madbouly, A. Lendlein, *Shape-Mem. Polym.* **2010**, *226*, 41.
[8] A. T. Neffe, B. D. Hanh, S. Steuer, A. Lendlein, *Adv. Mater.* **2009**, *21*, 3394.
[9] L. C. Chang, T. A. Read, *J. Met.* **1951**, *47*, 191.
[10] W. J. Buehler, J. V. Gilfrich, R. C. Wiley, *J. Appl. Phys.* **1963**, *34*, 1475.
[11] T. Xie, I. A. Rousseau, *Polymer* **2009**, *50*, 1852.
[12] J. S. Leng, X. Lan, S. Y. Du, W. M. Huang, N. Niu, S. J. Phee, Q. Yuan, *Appl. Phys. Lett.* **2008**, *92*, 014104; J. S. Leng, X. Lan, Y. Liu, S. Du, *Smart Mater. Struct.* **2009**, *18*, 074003.
[13] Q. Cao, P. Liu, *Polym. Bull.* **2006**, *57*, 889.
[14] A. Lendlein, H. Jiang, O. Junger, R. Langer, *Nature* **2005**, *434*, 879.
[15] R. Mohr, K. Kratz, T. Weigel, M. L. Gabor, A. Lendlein, *Proc. Natl. Acad. Sci. USA* **2006**, *103*, 3540.
[16] H. Koerner, G. Price, N. A. Pearce, M. Alexander, R. A. Vaia, *Nat. Mater.* **2004**, *3*, 115.
[17] A. Lendlein, R. Langer, *Science* **2002**, *296*, 1673.
[18] T. Xie, *Nature* **2010**, *464*, 267.
[19] X. Luo, P. T. Mather, *Adv. Funct. Mater.* **2010**, *20*, 2469 – 2656.
[20] M. Behl, I. Bellin, S. Kelch, W. Wagermaier, A. Lendlein, *Adv. Funct. Mater.* **2009**, *19*, 102 – 108; J. Zotzmann, M. Behl, D. Hofmann, A. Lendlein, *Adv. Mater.* **2010**, *22*, 3424; I. Bellin, S. Kelch, R. Langer, A. Lendlein, *Proc. Natl. Acad. Sci. USA* **2006**, *103*, 18043.
[21] J. Xu, J. Song, *Proc. Natl. Acad. Sci. USA* **2010**, *107*, 765.
[22] F. Cao, S. C. Jana, *Polymer* **2007**, *48*, 3790.
[23] P. Agarwal, H. Qi, L. A. Archer, *Nano Lett.* **2010**, *10*, 111.
[24] H. Y. Yu, D. L. Koch, *Langmuir* **2010**, *26*, 16801.
[25] R. Rodriguez, R. Herrera, L. A. Archer, E. P. Giannelis, *Adv. Mater.* **2008**, *20*, 4353.
[26] A. B. Bourlinos, R. Herrera, N. Chalkias, D. D. Jiang, Q. Zhang, L. A. Archer, E. P. Giannelis, *Adv. Mater.* **2005**, *17*, 234; A. B. Bourlinos, S. R. Chowdhury, R. Herrera, D. D. Jiang, Q. Zhang, L. A. Archer, E. P. Giannelis, *Adv. Func. Mater.* **2005**, *15*, 1285; A. B. Bourlinos, A. Stassinopoulos, D. Anglos, R. Herrera, S. H. Anastasiadis, D. Petridis, E. P. Giannelis, *Small* **2006**, *2*, 513.
[27] C. M. Yakacki, R. Shandas, D Safranski, A. M. Ortega, K. Sassaman, K. Gall, *Adv. Funct. Mater.* **2008**, *18*, 2428.
[28] P. T. Knight, K. M. Lee, H. Qin, P. T. Mather, *Biomacromolecules* **2008**, *9*, 2458.
[29] J. Brandrup, F. H. Immergut, *Polymer Handbook*, *3rd ed.*, Wiley, New York, **1989**.
[30] X. W. Lou, L. A. Archer, Z. C. Yang, *Adv. Mater.* **2008**, *20*, 3987.